

Positrons — an alternative probe to electron scattering

G.P. Karwasz^a

Faculty of Engineering, Trento University, 38050 Povo, Italy

Received 7 April 2004 / Received in final form 27 May 2005

Published online 17 August 2005 – © EDP Sciences, Società Italiana di Fisica, Springer-Verlag 2005

Abstract. Interaction of positrons with atoms and molecules differs from electron interaction due to the difference in polarity of the charge. This makes positrons an alternative tool to study atomic and molecular structure. Recent measurements of the total cross-sections for positron scattering at low energies on He, Ar, H₂, N₂, C₆H₆, C₆H₁₂, C₆H₇N carried out at Trento University [Karwasz et al., Acta Phys. Pol. **127**, 666 (2005)] are discussed and compared to electron scattering results. All measured total cross-sections exhibit an increase with decreasing positron energy in the limit of zero energy; H₂, N₂, Ar, show regions of constant cross-section which are a few eV-wide, characteristic of scattering on a hard-sphere potential. Helium shows two resonant structures much below the positronium formation threshold. They may be attributed to virtual positronium formation. In conclusion, positron scattering is complementary to electron scattering. The total cross-sections do not show Ramsauer minima but constant values, and new resonances appear.

PACS. 34.85.+x Positron scattering – 39.90.+d Other instrumentation and techniques for atomic and molecular physics

1 Electron scattering: benchmarks for quantum mechanics and atomic structure

Electron scattering contributed significantly to the formulation of quantum wave mechanics and gave new insight into atomic structure. The presence of minima in electron-scattering cross-sections, the so-called Ramsauer-Townsend (RT) effect [1], was discovered before de Broglie's wave hypothesis. The RT effect means that some gases, such as the heavier noble gases, become transparent for low energy electrons. This cannot be explained in classical mechanics terms, nor in old quantum mechanics terms, and was one of the first tests for quantum wave mechanics [2].

Following the wave mechanics, the total (elastic) cross-section σ_t can be described in terms of partial wave contributions as

$$\sigma_t = \frac{4\pi}{k^2} \sum_{l=0}^{\infty} (2l+1) \sin^2 \delta_l \quad (1)$$

where k is the wave number, l the angular momentum quantum number, and δ_l the shift of the wave-function phase caused by the presence of the scattering centre. The RT minimum occurs when the scattering potential

^a e-mail: karwasz@chemie.fu-berlin.de

Present address: Institut für Chemie-Physikalische und Theoretische Chemie, Freie Universität Berlin, 14195 Berlin, Germany.

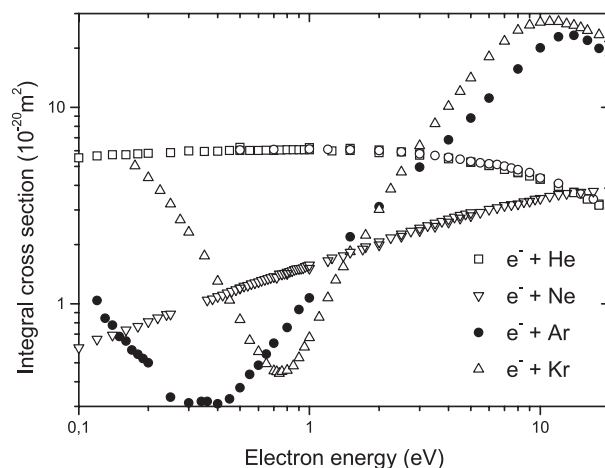


Fig. 1. Total cross-sections for electron scattering from noble gases. A Ramsauer-Townsend minimum is present in argon and krypton, no minimum is observed in He and Ne. For experimental points see the review [44].

is strong enough to bring the phase shift in the s -partial wave to a multiple of π . If this occurs at low energies where the phase shifts of higher partial waves are small, the cross-sections go almost to zero. The RT minimum occurs in electron scattering on Ar, Kr, Xe but not He and Ne (see Fig. 1).

A second crucial discovery were resonant structures in electron-scattering in gases not forming stable negative

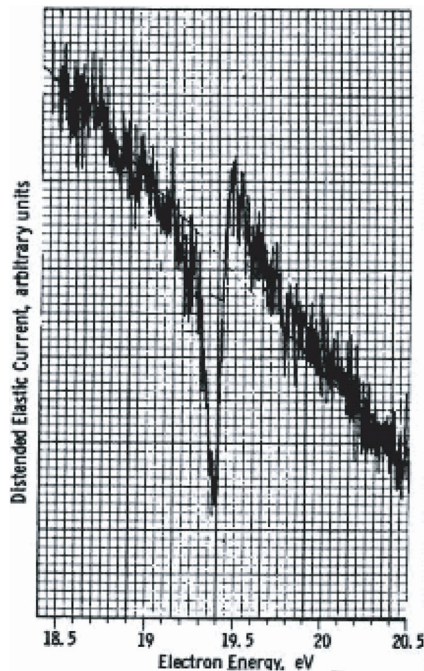


Fig. 2. Feshbach resonance structure observed in differential cross-section at 72° scattering angle, from reference [3], reproduced with permission from APS.

ions, such as He [3] and N_2 [4]. These resonances, i.e. temporary negative ions, can be classified into two types:

- (i) Feshbach resonances, with the incoming electron captured by the target in its electronically excited state, such as occurs for He at 19.36 eV [3], just below the first electronic-excitation threshold 2^3S_1 at 19.82 eV, see the original picture from Schulz's paper in Figure 2;
- (ii) shape resonances, with the incoming electron captured inside the effective scattering potential barrier, such as the resonance around 2.1 eV in N_2 [4].

Feshbach resonances in noble gases show up in differential cross-sections as sharp structures below thresholds for electronic excitation; their form in forward scattering is opposite to that in backward scattering, see example in Figure 3 for the $P_{3/2,1/2}$ doublet in Ar [5]. In terms of wave mechanics resonances consist in rapid changes of the wave phase superimposed on a slowly varying potential scattering. Shape resonances in molecules lead to selective enhancement of inelastic processes, such as vibrational excitation and electron attachments, and are visible also in total cross-sections, see Figure 4 for the $^2\Pi_g$ resonance in N_2 .

Positron scattering in the gas phase constitutes a sensitive test for atomic interactions. The static potential V_{stat} between the incoming electron and the fixed charge distribution in an atom is attractive. Positrons inside an atom experience a repulsive static interaction from the positive nucleus only partially screened by electrons. The polarization potential V_{pol} , i.e. the interaction with the dipole (or higher multipoles) induced by the incoming projectile,

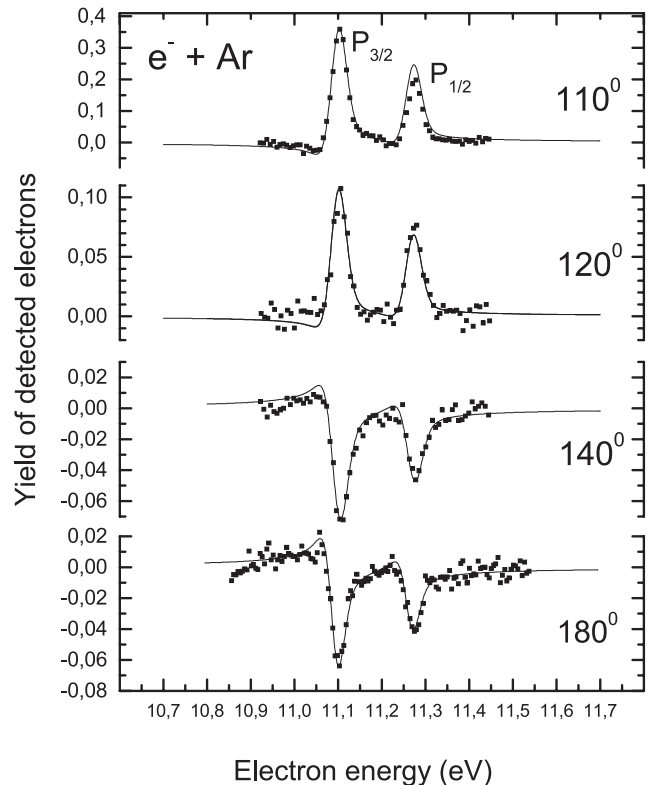


Fig. 3. Feshbach resonant structures for electron scattering from argon, with the electronic configuration of the temporary negative ion $3p^5(^2P_{3/2,1/2})4s^2(^1S)$, as seen in differential cross-sections. Experimental data adapted from reference [5], theory from reference [62].

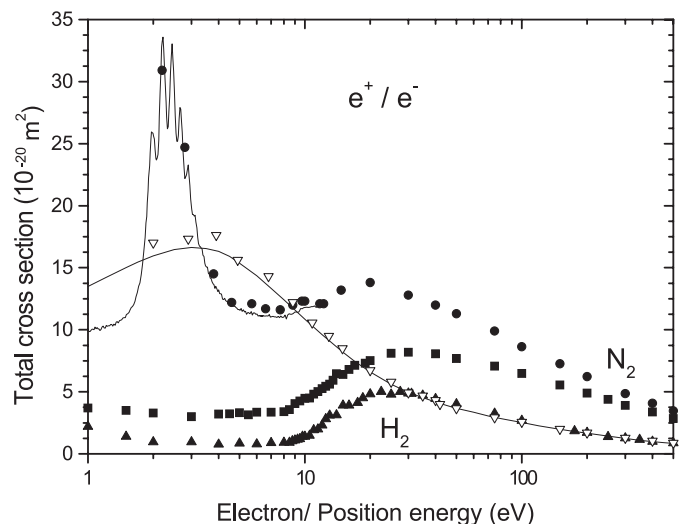


Fig. 4. Comparison of total cross-sections for electron and positron scattering from H_2 and N_2 . Experimental points are from reference [10]: open triangles, electron scattering from H_2 ; closed triangles, positron scattering from H_2 ; circles, electron scattering from N_2 ; squares, positron scattering from N_2 . Lines are: recommended values for H_2 [61] and measurements by Kennerly [63] for N_2 .

is attractive for both leptons but its form changes [6]. We write the total interaction for electrons in a symbolic way as

$$V^-(\mathbf{r}, \mathbf{v}) = -V_{stat}(\mathbf{r}, \mathbf{v}) - V_{pol}(\mathbf{r}, \mathbf{v}) - V_{ex}(\mathbf{r}, \mathbf{v}) \quad (2a)$$

and for positrons as

$$V^+(\mathbf{r}, \mathbf{v}) = +V_{stat}(\mathbf{r}, \mathbf{v}) - V_{pol}(\mathbf{r}, \mathbf{v}) \quad (2b)$$

where $V_{ex}(\mathbf{r}, \mathbf{v})$ is the exchange potential, reflecting Pauli's exclusion principle, and all potentials vary with the projectile distance \mathbf{r} and velocity \mathbf{v} . As seen from these equations, knowledge of both electron and positron cross-sections would allow us to derive single components of the scattering potential.

The opposite sign of the static interaction for positrons causes a kind of compensation between the two parts of the potential: small adjustments of these parts cause big differences in cross-sections. The weaker overall scattering potential makes the total cross-section generally lower for positrons than for electrons, see the example for nitrogen and hydrogen in Figure 4.

In the high energy region, the polarisation interaction, changing with the impact velocity, becomes relatively weaker. For the static potential, Born's approximation predicts equal cross-sections for positrons and electrons. The convergence of total cross-sections for positrons and electrons was observed for helium at about 200 eV and neon at 700 eV, see [7]. For hydrogen (see Fig. 4) and some molecules with a high polarisability, like CH_4 , SiH_4 , CCl_4 , C_2H_2 this convergence is observed at about 50 eV but only at 400 eV for CF_4 , see [7,8].

2 Positron scattering: open questions

Several questions remain open when comparing total cross-sections for electron and positron scattering:

1. convergence of the two cross-sections for heavier atoms in the high energy limit;
2. in the low energy region, early measurements in the limit of zero energy on targets such as Ar [9], N_2 [10], and hydrocarbons [11,12] indicated positron cross-sections rising with decreasing energy, but more recent experiments on molecular targets [13,14] indicate the contrary;
3. presence of Ramsauer's minimum, claimed in early measurements in He, Ne and Ar, but not in Kr and Xe, see [7];
4. existence of shape or Feshbach resonances — recent measurements indicate resonant-like huge enhancements of the positron annihilation rate in some hydrocarbons, like C_4H_{10} just below thresholds for vibrational excitation [15] but the interpretation is not clear; a systematic search for resonances at thresholds for electronic excitation in several targets was done in the same lab [16] with a negative result.

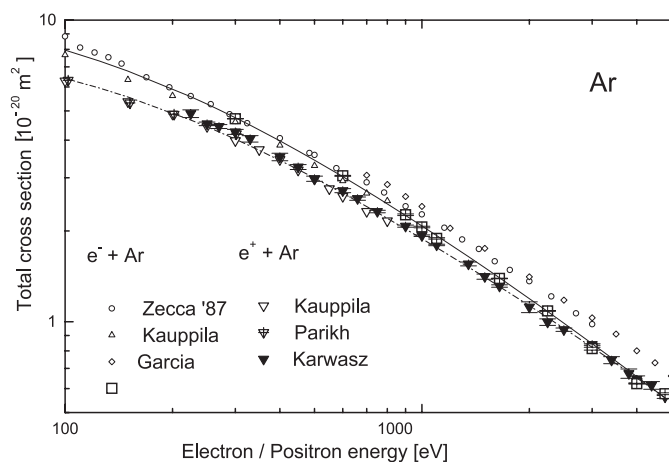


Fig. 5. Convergence of electron and positron total cross-sections in the high energy limit. Measurements from the Trento and Detroit lab for positrons and electrons and those of reference [71] for electrons are shown. Adapted from reference [18].

In spite of the importance for fundamental physics, only a few laboratories are active in the field of positron-gas phase scattering. We will refer to the most frequently cited here in a simplified manner: the Detroit group (Kauppila, Stein and collaborators [7,9]), San Diego (Surko and collaborators [15,16]), Tokyo (Sueoka, Kimura and collaborators [8,11–14]). Below, we discuss open issues in positron total cross-sections, comparing different experimental data, including the recent measurements from Trento University at high and low energies.

3 High energy convergence

In recent Trento experiments total cross-sections for positron scattering were measured in two energy regions: 0.4–20 eV [17] and 300–4000 eV [18]. The high energy set-up uses a transversal magnetic field to bend positrons (electrons) on a curvature of 20 cm radius. The vertical divergence of the positron beam is corrected by a sandwich-like set of electrodes. The apparatus is characterised by a moderately good angular resolution (1.0×10^{-3} sr) but does not use the retarding field analyser to discriminate against inelastically scattered projectiles in the forward direction. Therefore, the cross-sections in the high energy limit are underestimated, up to about 20% at 4 keV, as seen from comparison with electron cross-sections obtained on the same set-up but with a better (0.34×10^{-3} sr) angular resolution (see Fig. 5). The model using some analytical formula developed for electron scattering in this energy range [19] indicates that for Ar the two cross-sections converge but only in the high energy limit of 3–4 keV (see Fig. 5).

This convergence is less obvious for Kr [18]. Born's approximation requires that the scattering potential should be weak compared to the projectile kinetic energy. For Kr the interaction is stronger than for Ar and the limit of convergence is obtained at a higher energy. For SiH_4 ,

isoelectronic with Ar, the merging between positron and electron cross-sections is observed at about 200 eV [7]. Probably, for molecules the interplay between the static and polarisation component of the scattering potential makes positron and electron cross-sections converge at lower energies than for atoms.

4 Low-energy measurements

A new apparatus has been recently constructed in Trento for low energy (<20 eV) positron total cross-section measurements [17]. It works in a linear configuration and consists of two straight line segments connected with a 90° bend. In the first section positrons are extracted electrostatically from the thin W-monocrystal moderator and injected at 160 eV kinetic energy into the bend, which performs 1/100 $\Delta E/E$ energy discrimination. In the second part, a weak guiding magnetic field is used (0.9–1.1 mT). The scattering cell is 10 cm long and has an entrance and exit aperture of 1 mm diameter. Compared to the original design [20] the electrostatic potentials in the second part of the optics have been inverted from accelerating ones (the use of a remoderator was planned but turned out to be difficult in practice) to decelerating ones. Nevertheless, the counting rate is 10–100 e^+/s in the whole 0.4–20 eV range.

The geometrical angular resolution defined as a solid angle subtended by the exit aperture from the middle of the scattering cell is better by a factor of 50 than in the set-up of Sueoka [21]. However, it is not only the geometrical factor which determines the apparatus performance but also the interplay between the guiding magnetic field and the scattering cell apertures. The energy resolution in the Trento lab set-up is determined by three factors.

- (1) The bend cuts off any positrons outside the 1.6 eV — wide band.
- (2) Some monochromatic action is performed by the longitudinal magnetic field — positrons experience an integer number of gyrations (for example three at 2.4 eV scattering energy) inside the scattering cell. In test measurements, with an electron gun placed in front of the scattering cell, we observed in the $e^- + N_2$ total cross-section a resonant structure indicating a 130–150 meV resolution [20].
- (3) The energy width of positrons emitted from the moderator can be as low as 50 meV. We use 1 μm thick W(100) monocrystal moderator in transmission geometry; it is in-situ treated under high vacuum conditions (the ultimate pressure 7×10^{-9} mbar) at about 2700 K temperature in a complex procedure of degassing, annealing and recrystallization. The energy widths of positrons emitted from thick W foils (and in Venetian-blind configuration) is about 2 eV [22], the measurement of Canter and collaborators [23] with a 20 meV resolution on moderators similar to ours showed that the energy distribution is centred at 2.4 eV and is 40–50 meV wide, with only some low-energy tail.

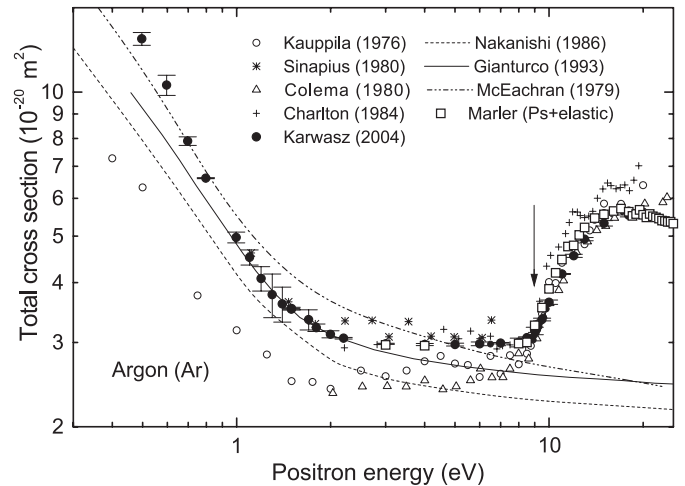


Fig. 6. Total cross-sections for positron scattering from argon. Experiment: Charlton et al. [64], Sinapius et al. [65], Coleman et al. [66], Kauppila et al. [9], Karwasz et al. [24], positronium formation cross-section [52] is plotted with the $2.95 \times 10^{-20} \text{ m}^2$ constant value added (assuming the additivity rule for partial cross-sections and a constant cross-section). Theory (elastic only): Gianturco et al. [28], McEachran et al. [29], Nakanishi and Schrader [30]. The arrow indicates the Ps formation threshold.

Unfortunately, no sharp structures are known in positron total cross-sections. Indirect evaluations of the energy resolution were done in reference [24] by precise measurements of the cross-section at the free positronium-formation threshold in Ar (see Fig. 6). In this way the energy scale shift by -2.4 eV has been determined, in agreement with the literature work function for tungsten moderators. Additionally, measurements of the rise of the beam intensity in the zero-energy limit (i.e. in retarding potential configuration) were performed [25]. These latter measurements indicate a 130 meV resolution with freshly treated moderator and 150 meV with several weeks old.

For electrons the energy resolution is probably much worse — secondary electrons emitted from the moderator show a large energy distribution, so probably the combined action of the bend and the magnetic lens is less effective. Measurements in the region of the RT minimum in Ar indicate that the resolution for electrons can be worse than 500 meV.

5 Total cross-sections in the zero-energy limit

The zero-energy limit is extremely interesting, as only few partial waves contribute to the cross-section. For electron scattering, a modified effective-range theory, considering the scattering on a polarisation potential solely, has been developed in the sixties [26]. It is still not verified with success even for noble gases, see reference [27] — precise data below 0.1 eV are needed. For positron scattering, due to a weaker potential, this limit can be higher, but data at low energies is generally lacking. The effective range

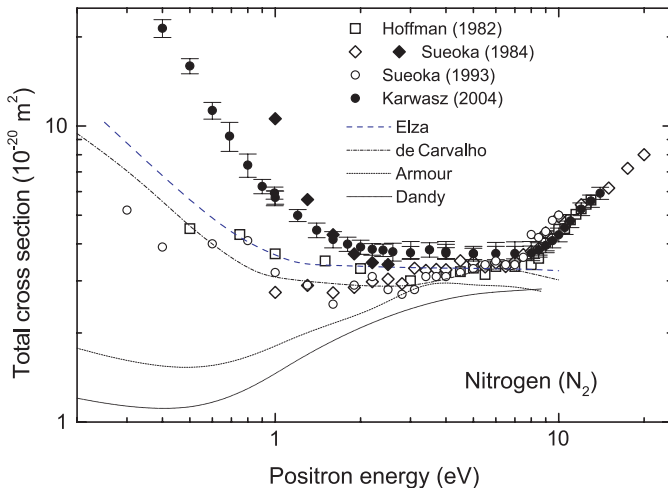


Fig. 7. Total cross-sections for positron scattering from nitrogen. Experiment: Hoffman et al. [10], Sueoka and Mori [21], Sueoka and Hamada [31], Karwasz et al. [24]. Full rhombuses are the experimental points of reference [21] corrected by us for the forward-angle resolution, using theoretical differential cross-sections of reference [33]. Theory (elastic): Elza et al. [6], de Carvalho et al. [33], Danby and Tennysson [35], Armour and Plummer [36].

theory states that in the zero energy limit the total cross-section tends to a constant value defined as

$$\sigma = 4\pi A^2 \quad (3)$$

where A is so-called scattering length.

In argon, the only measurements below 2 eV are those of the Detroit group [9] and the recent data from Trento [24] (see Fig. 6). Both sets indicate a rise in the limit of zero energy, varying approximately as $1/E$. Note that both sets agree well above the free-positronium threshold but differ by a factor of two below 1 eV. Possible reasons will be discussed below.

Theory also, independently of the model adopted, predicts a rise of the total cross-section in the limit of zero energy [28–30]; however, theories indicate also that the data from the Detroit group [7,9] are probably somewhat underestimated (see Fig. 6).

In nitrogen (see Fig. 7) measurements below 2 eV were performed both by the Detroit [10] and Tokyo [21,31] groups. In Figure 7 the data of Charlton et al. [32] starting at 2 eV, are omitted for clarity. Note also that the Tokyo data are normalised to those from Detroit [10]. The data from Trento [24] agree well with both sets above the positronium threshold but at 1 eV are higher by a factor of two. In order to understand the source of this discrepancy we have evaluated the correction due to the forward scattering error in the Trento and Tokyo experiments (both of them use about 0.9 mT magnetic field, but different apertures in collision chamber, 1 mm and 8 mm diameters, respectively). The correction is based on the fact that the magnetic field re-captures positrons scattered in the forward direction below a certain cut-off angle θ_1 . In the following formula, expressing the total cross-section in terms

of differential cross-sections $d\sigma/d\omega$, the forward-scattering error equals the first component of the sum below:

$$\sigma = 2\pi \left[\int_0^{\theta_1} \frac{d\sigma}{d\omega} \sin\theta d\theta + \int_{\theta_1}^{\pi} \frac{d\sigma}{d\omega} \sin\theta d\theta \right]. \quad (4)$$

Assuming all projectiles enter on the scattering cell axis, the angle θ_1 depends on the guiding magnetic field B , the projectile energy E and the radius ρ of the exit aperture, as follows

$$\theta_1 = \arcsin\left(\frac{eB\rho}{\sqrt{2mE}}\right) \quad (5)$$

(with e and m being positron charge and mass, respectively). Below a certain energy all positrons scattered into the forward hemisphere are counted as non-scattered, lowering the measured cross-section. For 4 mm aperture radius and 1 mT field this energy is 1.4 eV, for 0.5 mm radius as little as 0.02 eV.

The recent tabulated differential cross-sections for positron scattering in N_2 down to 0.001 eV [33] allowed us to calculate the forward-scattering correction in different experimental configurations. It turns out that in nitrogen the scattering is forward-centred down to 0.3 eV collision energy. In particular, at 1 eV the scattering into the forward hemisphere (at $\theta < 90^\circ$) constitutes as much as 3/4 of the total cross-section. The measured total cross-sections would be underestimated by a factor of four if all forward-scattered positrons are re-captured by the magnetic field. The correction in the Trento apparatus [24] is small: about 2–3% at 0.4 eV. In the Tokyo apparatus, the particular angular distribution of scattering makes the nitrogen total cross-sections [21] underestimated by a factor of about two at 1.4 eV, see full rhombuses in Figure 7. The corrected experimental points in N_2 from the Tokyo lab [21] would also indicate a rise of the cross-sections in the zero-energy limit, in a similar way to Ar.

Recent theories [6,33,34] indicate no RT minimum for nitrogen. However, as seen from Figure 7, the choice of a polarisation potential that is too weak [35,36] produces a spurious RT minimum.

Both for Ar and N_2 , the cross-sections at 1 eV are about a few \AA^2 . The Tokyo lab in early measurements for C_6H_6 [12] obtained cross-sections exceeding 100\AA^2 at 1 eV, rising in the limit of the zero energy. Those data agree with the recent theory but are in contrast with more recent determinations from the same lab [13] (see Fig. 8). Also the recent measurements from the Trento lab [37] indicate the rise of the cross-section in benzene in the limit of the zero energy (see Fig. 8).

We note that in the early Tokyo experiment [12] low values of the magnetic field were used (0.3 mT), which assured a small forward-scattering error. As shown for example in reference [38] for CCl_4 , the use of a high magnetic field (1 mT and above) in the Tokyo apparatus lowers significantly the measured cross-sections at energies below 5 eV. In benzene, the "final set" below 2.5 eV presented in reference [12] was measured with a weak (0.36 mT) field. Data obtained with the 0.9 mT field in that paper

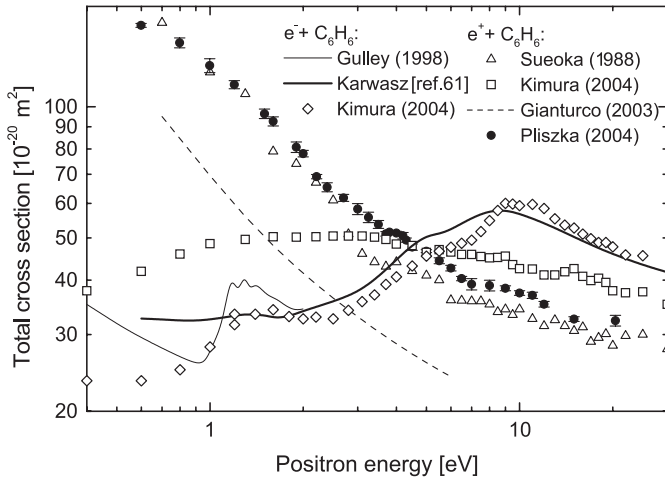


Fig. 8. Total cross-sections for positron and electron scattering from benzene. Positron data: Sueoka [12], Kimura et al. [13, 14], Pliszka et al. [37], theory by Occhigrossi and Gianturco [40]. Electron data: Kimura et al. [13, 14], Gulley et al. [69] at low energies and the values from the Landolt-Börnstein tables [61].

were lower by a factor of two at 1.5 eV, the data with the 2.3 mT field even descend in the zero energy limit.

The early Tokyo measurements show the zero-energy rise in the positron scattering also for other hydrocarbons, CH_4 , C_2H_4 , C_2H_6 [11] and C_2H_2 [39], the three latter being in agreement with the theory of Occhigrossi and Gianturco [40] who attributed the rising cross-sections to high polarisabilities of these target. Also in electron scattering on these targets the cross-section rises at low energies — in benzene at energies below 1 eV (see Fig. 8).

At Trento University [37] two more hydrocarbons were measured: aniline $\text{C}_6\text{H}_7\text{N}$ (the benzene ring with one NH_2 group instead of one H atom) and cyclohexane (C_6H_{12}) in which π carbon bonds are absent. Both molecules show a similar rise in the low energy limit (see Fig. 9); their polarisabilities are close to benzene ($72.2 a_0^3$, $81.7 a_0^3$, $73.6 a_0^3$ for benzene, aniline, cyclohexane, respectively).

Note that below 1 eV both benzene and cyclohexane show cross-sections tending to a constant value, as it is predicted by effective range theory [26]. Pliszka et al. [41] tried to fit the low energy dependence in cyclohexane and benzene with the following formula, being a modification of the theory

$$\sigma(E) = \frac{4\pi A^2}{\left[(1 - 0.5k^2 A r_0)^2 + k^2 A^2 + Ck \right]}. \quad (6)$$

In this formula, A is the scattering length A , r_0 the effective range, k wave number and C is an additional parameter introduced by us. The above expression approximates cross-sections in benzene and cyclohexane up to 1.5 eV within the statistical error bar. Parameters of the fit are given in Table 1. Note that the effective range r_0 for benzene is smaller (2.94 Å) than for cyclohexane (3.16 Å), which could be expected due to shorter bond lengths in benzene (1.395 Å) in comparison to cyclohexane (1.541 Å).

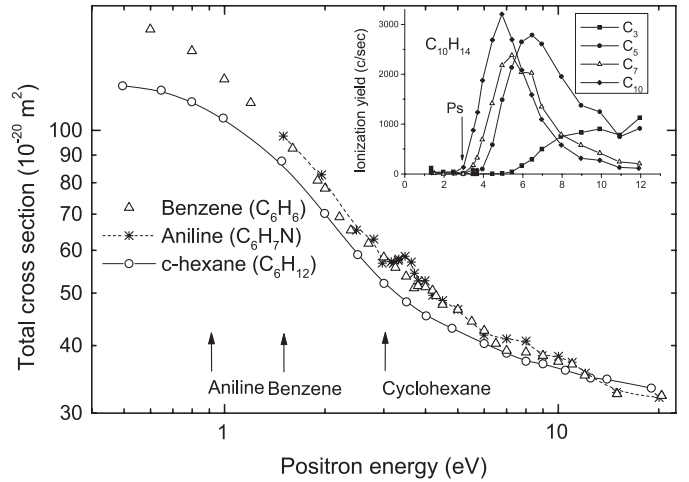


Fig. 9. Total cross-sections for positron scattering from benzene, aniline, cyclohexane from reference [37], lines are only for eye-guiding. Inset: ion yield from positron ionisation of $\text{C}_{10}\text{H}_{14}$, from reference [53]. Arrows show positronium formation thresholds.

Table 1. Comparison of the effective range fit parameters (Eq. (5)) for benzene and cyclohexane [41], A , r_0 and C are given Å, the value of the chi-square parameter of the fit is also given.

Parameter	Benzene	Cyclohexane
A	4.28	3.44
r_0	2.94	3.16
C	0.77	0.71
χ^2	1.01	1.07

6 Do positrons measure molecular diameters?

The tendency observed for hydrocarbons in the very low energy limit indicates the importance of the polarisation potential in positron-atom scattering. For Ar and N_2 no such levelling of the cross-section in the zero-energy limit is visible down to 0.4 eV (see Figs. 6 and 7). However, the recent measurements [24] (and comparison with earlier data) bring an even more interesting result in the energy region of a few eV, up to the positronium formation threshold.

The question of the RT minima in positron scattering was formulated already by the Detroit group [9, 42]. Unfortunately, little work was done afterwards, due to experimental difficulties in the very low energy range.

The main source of the error in positron measurements (once a high counting rate is assured) is the pressure evaluation. In the Trento lab [24] careful measurements were done in several series with constant pressure in Ar and N_2 , reducing the relative uncertainty to the statistical error bar (2–3%). These data are compared in Figure 10 with the preliminary data on H_2 [24]. All the data from Figure 10 indicate constant cross-section values, starting from about 2 eV for Ar and N_2 and about 4 eV for H_2 , up to the positronium formation threshold. At the threshold a steep rise is observed.

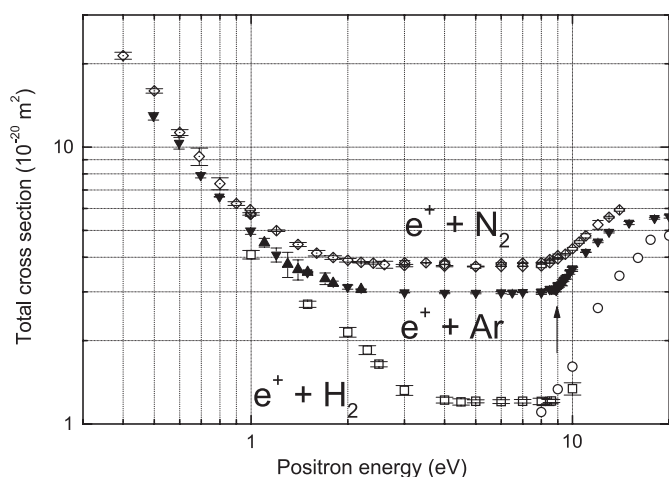


Fig. 10. Study of the hard-sphere hypothesis for total positron-scattering cross-sections on H_2 , N_2 , Ar, experimental data from reference [24]. Error bars correspond to statistical uncertainties; more points at a given energy mean several experimental runs. In H_2 the data above the positronium formation threshold are from reference [68].

We note that the same conclusion of constant cross-sections within the statistical error bar, can be drawn on the basis of the Detroit data for gases like Kr [43], CH_4 , SF_6 [44], and CO_2 [10] (see Fig. 11). In this figure statistical error bars quoted by the authors are given and three horizontal lines are drawn. The experimental points up to the positronium threshold lie on these lines, within the error uncertainty. The cross-sections start to rise only above the positronium formation threshold; some additional rise is seen in CO_2 after the ionisation threshold. In the same graph we show the total cross-section for electron scattering on Kr, see the review [45]. One sees immediately, that RT minima in electron scattering are very narrow structures if compared to wide plateaus in positron cross-sections.

That the total cross-section is independent of energy is a rather surprising result, as any scattering potential, including the hard-sphere, shows some energy dependence according to quantum wave mechanics. The same is valid for classical mechanics, apart from the billiard-like, hard-sphere scattering. It seems that positrons with a sufficiently high energy (i.e. of a few eV) encounter a hard-sphere (repulsive) potential. On the other hand, absolute values of the cross-sections in this energy region are a few \AA^2 , i.e. of the expected atomic or molecular dimensions.

The question of atom dimensions is one of the first lessons in Atomic Physics. Dushman and Lafferty [46] tabulated different values for atomic and molecular radii R obtained from: (1) gas-phase viscosity measurements analysed by two different models, (2) electron-scattering total cross-sections at an arbitrary chosen energy of 30 eV, taking simply $\sigma = \pi R^2$, (3) geometrical diameters derived from the density of liquefied gases.

As seen from the table, diameters obtained by all methods differ significantly. The atomic diameter in He obtained from van der Waals coefficients is higher than in Ne

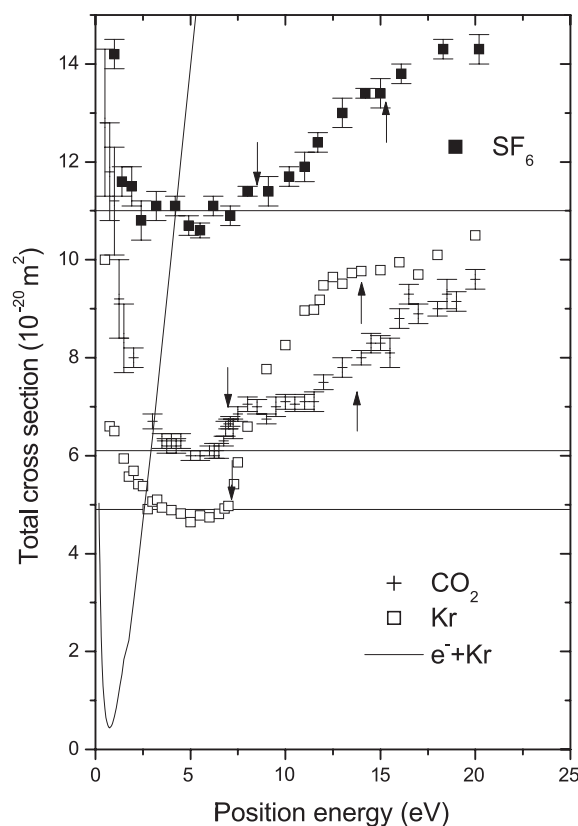


Fig. 11. Study of the hard-sphere hypothesis for total positron-scattering cross-sections on Kr [43], CO_2 [10], SF_6 [44]. Horizontal lines are drawn for reference, note wide energy regions where the cross-section is equal to these lines within the statistical error bar. Thin line is $e^- + \text{Kr}$ cross-section, data from the review [45]. Arrows from above show the positronium formation threshold, from below the ionisation threshold.

and Ar, similarly to the diameter from the liquid density. The liquid density gives a higher diameter for H_2 than for Ar and CO_2 . Viscosity models seem to present less contradictions, although the two models give quite different absolute values. Electron scattering, apart from the fact that 30 eV is an arbitrary chosen energy, also gives some unexpected results, such as the CO_2 molecule diameter lower than that for Kr atom.

The fact that positron-scattering cross-section is constant over a wide energy range induced us to calculate hard-sphere diameters from these constant values, using the classical geometrical expression $\sigma = \pi R^2$. Results are given in the last column of Table 2. These data show the scaling which can be expected intuitively, in a rising order: He, Ne, H_2 , $\text{Ar} \approx \text{N}_2$, $\text{Kr} \approx \text{CO}_2$, SF_6 . The helium diameter is revealed to be the smallest, as expected from quantum mechanics calculations. The hydrogen molecule radius (0.62 \AA) is 20% higher than Bohr's radius. As can also be seen also from Kauppila and Stein' review [7] numerous other targets, Xe, CO, N_2O , CH_4 , SiH_4 , C_2H_4 show regions of constant cross-section, below positronium formation threshold, allowing us to deduce the molecular radii. In heavier targets (Xe, SiH_4) the low-energy descent

Table 2. Comparison of the molecular diameters $2R$ (in Å) obtained with different experimental methods: viscosity measurements (δ_0, δ_m), van der Waals interactions (b), liquid density measurements (d) and electron collision experiments (total cross-sections at 30 eV), all from reference [46]. We compare these data with diameters derived from positron total cross-sections at low energies, using recent results from Trento lab (He, Ar, N₂, H₂) and Detroit lab (Ne, Kr, CO₂, SF₆). Note that Detroit data are usually lower than Trento ones, by about 15–20% in Ar. Electron collisions data are from the review [45].

Atom/ molecule	From δ_0	From δ_m	From b	From d	Electron collisions	Positron collision
He	2.18	1.69	2.66	4.21	1.7	0.40
Ne	2.6	2.16	2.38	3.4	2.2	1.06
Ar	3.67	2.42	2.49	4.15	4.3	1.96
Kr					4.9	2.5
H ₂	2.75	2.1	2.67	4.19	2.5	1.25
N ₂					4.0	2.04
CO ₂	4.65	3.32	3.24	4.05	4.7	2.7
SF ₆					6.1	3.7

of the cross-sections extends very near to the Ps threshold so the constant part of the cross-section is only a few eV-wide. Also for these heavier targets the radii derived show the expected scaling.

In N₂, the recent measurements [49] of the electronic charge distribution with ultrafast laser light scattering show that the highest occupied orbital has a maximum of the charge distribution at about 1–1.1 Å. This value coincides with the radius presently deduced from positron scattering, see Table 2.

Classical models for scattering on a hard-sphere potential predict isotropic angular distributions. As shown by Detroit experiments for Ar [7] and N₂ [47] this is not the case — differential cross-sections vary with the scattering angle. Compared to electron scattering [62], positron cross-sections show a weak dependence on angle — this is clearly visible for Ar, see Figure 12a. Differential cross-sections in N₂ remain almost identical at 5.25 and 6.75 eV, i.e. below the Ps formation threshold but change significantly above this threshold.

Quantum mechanics predicts for hard-sphere scattering the cross-section value of $4\pi R^2$ in the limit of zero energy (Eq. (5)) and the value of $2\pi R^2$ in the limit of high energies [48]. The experimental differential cross-sections at low energies in N₂ and Ar (Fig. 12) show a dependence resembling somewhat the rainbow-like pattern predicted by quantum mechanics for a rigid sphere, but absolute values are not correct.

To summarise, the general pattern of total cross-sections for positron scattering on targets such as, Ar, Kr, Xe, N₂, H₂, CO₂, SF₆ is as follows:

(1) in the very low energy range the scattering is dominated by long-range polarisation forces, causing the cross-sections to be constant in the zero energy limit and then fall with rising energy, in agreement with the modified effective-range theory;

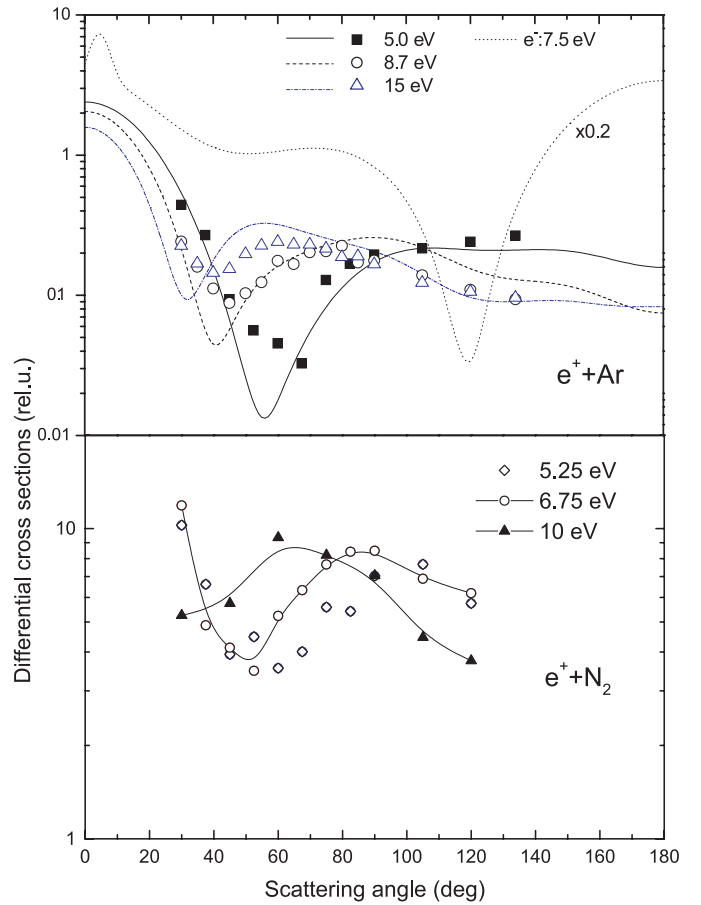


Fig. 12. (a) Differential cross-sections for positron scattering on argon, relative data from reference [7] and private information. Experimental relative data have been normalized to the theory, reference [29]. Theoretical differential cross-sections for electrons, reference [62] are shown for comparison. (b) Differential cross-sections for positron scattering on nitrogen, relative data from reference [47]. The 5.25 eV and 6.75 eV curves (the region of constant total cross-section, see Fig. 10) differ from that at 10 eV, i.e. above the Ps-formation threshold.

(2) at higher energies positrons penetrate inside the electronic charge and experience a strong (repulsive) force at a distance corresponding to the expected position of the valence electrons. Alternatively, some well-localized quasi-absorption process at this distance needs to be hypothesized.

7 Positronium-formation cross-section

The total cross-section can be considered as a sum of all partial processes, i.e. elastic, ionisation etc. or as a kind of *constant* of scattering. The latter idea comes from the dispersion relation in optics, which relates absorption and transmission properties over the range of the whole spectrum. For electron (positron) scattering the dispersion relation compares the elastic differential cross-section at zero angle with the integral of the total cross-sections from zero energy to infinity. For electron scattering the

problem was extensively studied by de Heer and collaborators [50], but no conclusion on the validity of the dispersion relation was achieved for noble gases. For positron scattering, Kauppila et al. [51] concluded that the dispersion relation holds for He, Ne and probably also for argon. A new methodology of differential cross-section measurements has recently been developed in San Diego. This should allow a more precise validation of the dispersion relation, but the data obtained are still far from being complete, see [15].

The first approach to total cross-sections, on adding partial cross-sections, is more intuitive. In Figure 6 we compare the recent precise measurements of positronium formation in argon from San Diego [52] with the total cross-sections. In this figure, assuming the additivity rule, we add a constant value (2.95 \AA^2), corresponding to the elastic cross-section at 8 eV, to the positronium-formation cross-sections. The agreement between the summed and the experimental total cross-section is very good, within the error bars. This comparison indicates that the rise of the total cross-section in Ar above 9 eV can be exclusively attributed to the free positronium channel. No such precise data on positronium formation exist for N_2 and H_2 .

The Detroit data for Kr, CO_2 , SF_6 (see Fig. 11) also indicate another interesting dependence. In gases in which electron attachment is possible, i.e. with stable negative (parent or dissociated) ions and high cross-sections for this process (such as SF_6 , CO_2 , see [45]), the rise of the total cross-section above the Ps formation threshold is much lower than in the gases which do not attach electrons, like Kr. For example, in CO_2 the rise of the cross-sections above the Ps threshold is only $1 \times 10^{-16} \text{ cm}^2$ while in Kr it is as much as $5 \times 10^{-16} \text{ cm}^2$.

8 Positronium formation in hydrocarbons

The positron-scattering total cross-section in benzene is almost $200 \times 10^{-20} \text{ m}^2$ at 0.6 eV. The simplest explanation for such a huge value would be the capture of an incoming positron inside the benzene ring. Substituting one hydrogen in the benzene ring with a functional group modifies the electronic charge density and the cross-section should change. This was the reason for measurements on aniline (with the NH_2 substitution group). Surprisingly, the cross-sections in aniline is almost identical to that in benzene. The only difference clearly outside the combined error bar is the small maximum at about 3.5 eV. It resembles the small hump visible in benzene data at about 4 eV both in the Tokyo [12] and Trento [37] measurements (see Fig. 9).

The most probable hypothesis for these cusps is the formation of positronium. Positronium formation thresholds are very low both for benzene (2.4 eV) and aniline (1.9 eV). Sueoka [12] in benzene, using a high magnetic field evaluated the positronium formation cross-section to be as much as $6 \times 10^{-16} \text{ cm}^2$ at 4.4 eV.

The observed maximum in aniline at 3.5 eV is about $8 \times 10^{-16} \text{ cm}^2$, more clearly visible than the hump in benzene. This could be a chemical effect, probably due to

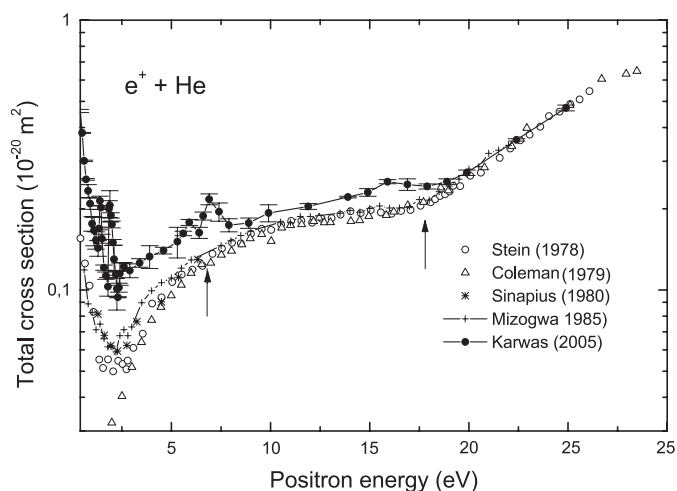


Fig. 13. Total cross-sections for positron scattering on helium. Experimental data are shown only: Stein et al. [55], Coleman et al. [69], Sinapius et al. [65], Mizogawa et al. [22], Karwasz et al. [25]. The arrows show the energy of $1/2$ Rydberg and the free-Ps threshold.

positronium formation in the two different spin states (ortho and para). Such an effect has recently been observed for CO_2 and O_2 by the Detroit group [54]. They suggested some selective positron attachment to inner-shell electrons. A similar hypothesis could be formulated on differences between benzene and cyclohexane cross-sections: the positron attachment to a specific site. But, as suggested by Laricchia, it could also be a kinematical effect, due to the lower Ps formation threshold in aniline than in benzene. We observe from the positron-impact ionisation studies in molecules (C_4H_{10}) [53] that the cross-section for the parent-ion formation reaches a higher maximum and at a lower energy than the formation of the dissociated ions, see the insert in Figure 9. Further work is needed to discern between the two hypothesis (kinematical effect or selective positron capture) in hydrocarbons.

9 Helium: apparently the most simple case

The early measurements from the Detroit lab [55] indicated very low, almost constant values of the $e^+ + \text{He}$ total cross-section, between 1.5 eV and 5 eV. Applying the geometrical formula this would yield a radius as small as 0.34 \AA . Measurement from the Trento laboratory [25] aimed to verify this low value. Similarly to argon, hydrogen and nitrogen, the agreement between the Trento and Detroit data is excellent above the positronium formation threshold but at low energies Trento data in He are higher by a factor of almost three (see Fig. 13). However, no experimental details are available in reference [55] which would allow some a-posteriori correction due to the forward scattering, as was possible in the case of N_2 .

Another specific feature of helium positron-scattering resulting from early measurements, is the rise of the total cross-section just at energies above a few eV, far below the positronium formation threshold (17.8 eV). Out of targets

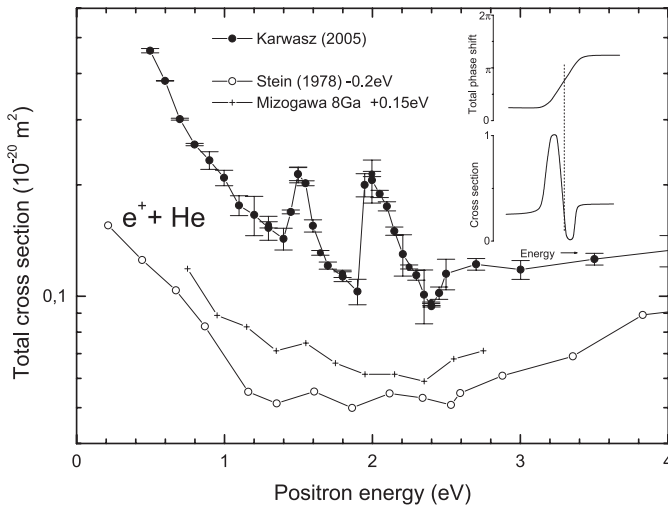


Fig. 14. Detail of the low energy range in He. Experimental points are from reference [25], compared to those from the Detroit lab [55] and by Mizogawa et al. [22] obtained with the 0.8 mT magnetic field. For the sake of the comparison with the Trento data [25], the Detroit points have been shifted on this figure by -0.2 eV and Mizogawa et al.'s data by $+0.15$ eV. The energy error in reference [25] is about ± 0.1 eV. Lines are drawn as a guide to the eye. The insert shows predicted, see reference [70], shape of resonant structure for the $+\pi$ phase shift due to a resonance, superimposed on a small positive shift due to potential scattering.

reviewed by Kauppila and Stein [7] only Ne and O₂ show such a dependence. The rise of the cross-section in He seems to arrive at a kind of plateau at the free-positronium threshold, then the cross-sections rise further (see Fig. 13). Somewhat similar, several eV-broad maxima are present in electron scattering on CH₄ and other hydrocarbons and are usually attributed to short-lived resonances, see reference [45].

Resonant structures are predicted theoretically in helium (and H) but just below the free-Ps formation threshold [56]. In fact, a rather broad structure has been observed at about 17 eV in the Trento measurements [25]. Another structure has been observed at about 7 eV (see Fig. 13) and the most prominent, between 1.4–2.6 eV (see Fig. 14). This latter appears to be a double peak, with a sharp rise and somewhat slower fall. The rise in the second peak (at 1.9 eV) is very rapid, within 0.1 eV.

In He measurements in the Trento lab several precautions were taken to exclude experimental artefacts: a check on the independence of the cross-sections to the magnetic field and pressure, repeated measurements with a random choice of energies, improved statistics on some points; the gas purity was checked using a mass spectrometer after measurements. The resonant structures are independent on measurement conditions.

Only two experiments [22,55] in He have been performed before below 2 eV. The measurements of the Detroit group [55] date to the seventies, but were performed with a good energy resolution — they used ¹¹B proton-irradiated source of positrons and they showed a

0.1 eV-broad energy distribution from the intrinsic B moderator. However, the bent configuration and rather large exit apertures (4.8 mm in diameter) probably led to a poor forward-scattering resolution. On the other hand, in the experiment of Mizogawa et al. [22] somewhat smaller (4 mm in diameter) apertures and a weak (0.8–1.3 mT) magnetic field were used but the energy resolution was probably poor, due to the use of a thick tungsten ribbon as moderator, in Venetian-blinds configuration. Furthermore, the early measurements could demonstrate some shift in energy scale — the Detroit machine had no direct energy determination, the work function of boron is unknown and Mizogawa's energy calibration against the 19.36 eV Schulz's resonance [3] gave a value different by 0.15 eV. In Figure 14 we show that, probably, some traces of the resonant structures in e^+ +He were already seen by these two groups, but the indications are not clear. More measurements would be needed.

The theory of atomic resonances predicts some characteristic shapes, according to the resonant phase shift (positive or negative) and to the phase shift from non-resonant (potential) scattering. The two structures in Figure 14. follow the shape predicted by a $+\pi$ change of the phase shift superimposed on a small, positive phase shift from the potential (i.e. non resonant) scattering. Theories differ somewhat on exact calculation of the potential-scattering shift in He, but on average (see discussion in [57]), they predict at 3 eV ($k = 0.38$ a.u.) the s -wave phase shift of about $+0.05$ rad descending with k and the p -wave phase-shift is about $+0.03$ rad rising with k . These values would yield the shape of the resonant structures as shown in Figure 14. Note that the structures from Figure 14 have an inverted shape compared to the e^- +He structure, as seen by Schulz [3] in the signal of electrons scattered at the angle of 72° (see Fig. 2). Note also that in the e^- +He scattering the structure inverts if observed at backward angles.

However, the most puzzling question is about the inelastic processes possibly involved in the e^+ +He resonances at 1.4–2.6 eV — no channel is open at such low energies. A hint comes from Gribakin and King [58] who showed that the theoretical cross-section is underestimated in its minimum by a factor of three, unless the virtual positronium formation channel is included. Our hypothesis is that the resonant structures in Figures 13 and 14 mark thresholds for the formation of the virtual positronium in two spin states. The term "virtual positronium" means that the incoming positron attaches temporarily (for about 10^{-14} s) to one of He electrons and performs some gyrations together, before being detached. These resonances can be also interpreted as a molecule, consisting of the He⁺ ion and the Ps atom.

We find no theoretical indications for these structures in calculations of cross-sections. The four-body static problem (He²⁺, $2e$, e^+) yields energy eigenvalues of 0.544 eV, 2.451 eV, 6.428 eV, 12.722 eV and 17.773 eV [59]. A basis of 768 explicitly correlated Gaussian spatial functions, optimised for the lowest quartet state [60] were used in these calculations. These eigenvalues would

roughly correspond to the positions of resonance observed, but still do not explain their presence in the scattering experiments.

10 Conclusions

In conclusion, comparison of different positron data in noble gases and molecules such as H_2 , N_2 , CO_2 , SF_6 shows that total cross-sections, unlike electron scattering, show some simple patterns:

- (1) a decrease with energy — for atoms (Ar, He) and simple molecules (H_2 , N_2) in the range from zero up to a few eV and for complex molecules up to about 10 eV;
- (2) a constant value up to the positronium formation threshold in atoms and simple molecules;
- (3) a steep rise at the free-Ps threshold that can be totally attributed to the Ps-formation process.

Helium shows a rise of the cross-section much before the free-Ps threshold and sharp resonant structures.

The problems requiring urgent theoretical interpretation are:

- (1) a model to be applied (quantum mechanics vs. classical) for explaining *constant* cross-sections for low-energy positron scattering on atoms and small molecules;
- (2) the possibility of virtual positronium formation in targets such as He.

Positron atomic spectroscopy turns out to be totally alternative to electron scattering: total cross-sections do not show Ramsauer-Townsend minima but constant values, and resonances appear in new channels, not existing for electrons.

The experimental results cited as Trento data come from the measurements performed by the team: Prof. A. Zecca, Prof. R.S. Brusa, Dr. D. Pliszka and G.K. Note the separate papers in which these data are discussed in detail. My stay at Freie Universität Berlin was possible thanks to the European Science Foundation, EIPAM program; special thanks to Prof. Eugen Illenberger for the hospitality. I thank Prof. M. Zubek for his tabulated values of Ar resonance and Prof. C. Surko and Dr J. Marler for sending their Ps cross-sections in Ar. The theoretical calculations cited in Section 9 were performed by Dr K. Strasburger, I acknowledge his help and discussions. I acknowledge also discussions with prof. F. Gianturco, G. Laricchia, S. Buckman. This work is dedicated to my wife, Maria.

References

1. C. Ramsauer, Ann. Phys. (Leipzig) **66**, 546 (1921)
2. J. Holtsmark, Z. Phys. **44**, 437 (1929)
3. G.J. Schulz, Phys. Rev. Lett. **10**, 104 (1963)
4. G.J. Schulz, Phys. Rev. **125**, 229 (1962)
5. M. Zubek, B. Mielewska, J. Channing, G.C. King, F.H. Read, J. Phys. B **32**, 1351 (1999)
6. B.K. Elza, T.L. Gibson, M.A. Morrison, B.C. Saha, J. Phys. B **22**, 113 (1989)
7. W.E. Kauppila, T.S. Stein, Adv. At. Mol. Opt. Phys. **26**, 1 (1990)
8. M. Kimura, O. Sueoka, A. Hamada, Y. Itikawa, Adv. Chem. Phys. **111**, 537 (2000)
9. W.E. Kauppila, T.S. Stein, G. Jesion, Phys. Rev. Lett. **36**, 580 (1976)
10. K.R. Hoffman, M.S. Dababneh, Y.-F. Hsieh, W.E. Kauppila, V. Pol, J.H. Smart, T.S. Stein, Phys. Rev. A **25**, 1393 (1982)
11. O. Sueoka, S. Mori, J. Phys. B **19**, 4035 (1986)
12. O. Sueoka, J. Phys. B **21**, L631 (1988)
13. C. Makochekanwa, O. Sueoka, M. Kimura, Phys. Rev. A **68**, 32707-1 (2003)
14. M. Kimura, C. Makochekanwa, O. Sueoka, J. Phys. B **37**, 1461 (2004)
15. J.P. Sullivan, S.J. Gilbert, J.P. Marler, L.D. Barnes, S.J. Buckman, C.M. Surko, Nucl. Instr. Meth. B **192**, 3 (2002)
16. J.P. Sullivan, S.J. Gilbert, S.J. Buckman, C.M. Surko, J. Phys. B **34**, L467 (2001)
17. G. Karwasz, R.S. Brusa, M. Barozzi, A. Zecca, Nucl. Instr. Meth. B **171**, 178 (2000)
18. G.P. Karwasz, M. Barozzi, R.S. Brusa, A. Zecca, Nucl. Instr. Meth. B **192**, 157 (2002)
19. G.P. Karwasz, R.S. Brusa, A. Piazza, A. Zecca, Phys. Rev. A **59**, 1341 (1999)
20. E. Rajch, A. Zecca, R.S. Brusa, S. Mariazzi, G.P. Karwasz, Int. Soc. Opt. Engineer. Proc. SPIE **5258**, 190 (2003)
21. O. Sueoka, S. Mori, J. Phys. Soc. Jap. **53**, 2491 (1984)
22. T. Mizogawa, Y. Nakayama, T. Kawaratami, M. Tosaki, Phys. Rev. A **31**, 2171 (1985)
23. G. Amarendra, K.F. Canter, D.C. Schoepf, J. Appl. Phys. **80**, 4660 (1996)
24. G.P. Karwasz, D.P. Pliszka, R.S. Brusa, Phys. Rev. A (submitted)
25. G.P. Karwasz, D.P. Pliszka, A. Zecca, R.S. Brusa, Nucl. Instr. Meth. B (in press)
26. T.F. O'Malley, Phys. Rev. **130**, 1020 (1963)
27. S.J. Buckman, J. Mitroy, J. Phys. B **22**, 1365 (1989)
28. F.A. Gianturco, A. Jain, J.A. Rodriguez-Ruiz, Phys. Rev. A **48**, 4321 (1993)
29. R.P. McEachran, A.G. Ryman, A.D. Stauffer, J. Phys. B **12**, 1031 (1979)
30. H. Nakanishi, D.M. Schrader, Phys. Rev. A **34**, 1823 (1986)
31. O. Sueoka, A. Hamada, J. Phys. Soc. Jap. **62**, 2669 (1993)
32. M. Charlton, T.C. Griffith, G.R. Heyland, G.L. Wright, J. Phys. B **16**, 323 (1983)
33. C.R.C. de Carvalho, M.T. do N. Varela, M.A.P. Lima, E.P. da Silva, J.S.E. Germano, Nucl. Instr. Meth. B **171**, 33 (2000)
34. F.A. Gianturco, P. Paoletti, J.A. Rodriguez-Ruiz, Z. Phys. D **36**, 51 (1996)
35. G. Danby, J. Tennyson, J. Phys. B **24**, 3517 (1991)
36. E.A.G. Armour, M. Plummer, J. Phys. B **24**, 4463 (1991)
37. G.P. Karwasz, D. Pliszka, R.S. Brusa, C. Perazzolli, Acta Phys. Pol. **107**, 666 (2005)
38. A. Hamada, O. Sueoka, Appl. Surf. Sci. **85**, 64 (1995)
39. O. Sueoka, S. Mori, J. Phys. B **22**, 963 (1989)
40. A. Occhigrossi, F.A. Gianturco, J. Phys. B **36**, 1383 (2003)
41. *5th FAMO Workshop on Atomic, Molecular Physics and Optics*, Proc. SPIE **5849**, 242 (2005), edited by D. Pliszka, R.S. Brusa, G.P. Karwasz, Jurata, Poland, 17-19 September 2004 (The International Society for Optical Engineering, in press)

42. W.E. Kauppila, T.S. Stein, G. Jesion, Phys. Rev. Lett. **36**, 580 (1976)
43. M.S. Dababneh, W.E. Kauppila, J.P. Downinh, F. Lapierrere, V. Pol, J.H. Smart, T.S. Stein, Phys. Rev. A **22**, 1872 (1980)
44. M.S. Dababneh, Y.-F. Hsieh, W.E. Kauppila, C.K. Kwan, S.J. Smith, T.S. Stein, M.N. Uddin, Phys. Rev. A **38**, 1207 (1988)
45. A. Zecca, G.P. Karwasz, R.S. Brusa, Riv. Nuovo Cimen. **19**(3), 1 (1996); G.P. Karwasz, A. Zecca, R.S. Brusa, Riv. Nuovo Cim. **24**(1), 1 (2001); G.P. Karwasz, A. Zecca, R.S. Brusa, Riv. Nuovo Cim. **24**(4), 1 (2001)
46. S. Dushman, J.M. Lafferty, *Scientific Foundations of Vacuum Technique* (J. Wiley & Sons, New York, 1962)
47. D.A. Przybyla, W. Addo-Asah, W.E. Kauppila, C.K. Kwan, T.S. Stein, Phys. Rev. **60**, 350 (1999)
48. N.F. Mott, H.S.W. Massey, *Theory of Atomic Collisions* (Clarendon, Oxford, 1965)
49. J. Itatani, J. Levesue, D. Zeidler, Hiromichi Niikura, H. Pépin, J.C. Kieffer, P.B. Korkum, D.M. Villeneuve, Nature **432**, 867 (2004)
50. F.J. de Heer, M.R.C. McDowell, R.W. Wagenaar, J. Phys. B **10**, 1945 (1977)
51. W.E. Kauppila, T.S. Stein, J.H. Smart, M.S. Dababneh, Y. K. Ho, J. P. Downing, V. Pol, Phys. Rev. A **24**, 725 (1981)
52. J.P. Marler, J.P. Sullivan, C.M. Surko, Phys. Rev. A **71**, 022701 (2005)
53. Jun Xu, L.D. Hulet Jr, T.A. Lewis, D.L. Donohue, S.A. McLuckey, G.L. Glish, Phys. Rev. A **47**, 1023 (1993)
54. W.E. Kauppila, E.G. Miller, H.F.M. Mohamed, K. Pipinos, T.S. Stein, E. Surdutovich, Phys. Rev. Lett. **93**, 113401 (2004)
55. T.S. Stein, W.E. Kauppila, V. Pol, J.H. Smart, G. Jesion, Phys. Rev. A **17**, 1600 (1978)
56. J.W. Humberston, J. Phys. B **11**, L343 (1978); P. Van Reeth, J.W. Humberston, Nucl. Instr. Meth. B **171**, 106 (2000)
57. D. De Fazio, F.A. Gianturco, J.A. Rodriguez-Ruiz, K.T. Tang, J.P. Toennies, J.Phys. B **27**, 303 (1994)
58. G.F. Gribakin, W.A. King, J. Phys. B **27**, 2639 (1994)
59. K. Strasburger, private communication
60. K. Strasburger, J. Phys. B **37**, 2211 (2004)
61. G.P. Karwasz, A. Zecca, R.S. Brusa, in: *Photon and Electron Interaction, with Atoms, Molecules and Ions*, Chapter VI.1 Electron Scattering with Molecules. Total, Landolt-Börstein New Series (Springer-Verlag, Berlin, Heidelberg, 2003), Volume I/17, pp. 6.1-6.51
62. J.E. Sienkiewicz, W.E. Baylis, J. Phys. B **20**, 5145 (1987)
63. R.E. Kennerly, Phys. Rev. A **21**, 1876 (1980)
64. M. Charlton, G. Laricchia, T.C. Griffith, G.L. Wright, G.R. Heyland, J. Phys. B **17**, 4945 (1984)
65. G. Sinapius, W. Raith, W.G. Wilson, J. Phys. B **13**, 4079 (1980)
66. P.G. Coleman, J.D. McNutt, L.M. Diana, J.T. Hutton, Phys. Rev. A **22**, 2290 (1980)
67. R.J. Gulley, S.L. Lunt, J.P. Ziesel, D. Field, J. Phys. B **31**, 2735 (1998)
68. A. Deuring, K. Floeder, D. Fromme, W. Raith, A. Schwab, G. Sinapius, P.W. Zitzewitz, J. Phys. B **16**, (1983) 1633
69. P.G. Coleman, J.D. McNutt, L.M. Diana, J.R. Burciaga, Phys. Rev. A **20**, 145 (1979)
70. G.J. Schulz, Rev. Mod. Phys. **45**, 378 (1973)
71. G. Garcia, F. Arqueros, J. Campos, J. Phys. B **19**, 3777 (1986)